COMPRESSION AND RECONSTRUCTION METHODOLOGY FOR NEURAL SIGNALS BASED ON PATCH ORDERING INPAINTING FOR BRAIN MONITORING

Sebastian Schmale, Heiner Lange, Benjamin Knoop, Dagmar Peters-Drolshagen and Steffen Paul

Institute of Electrodynamics and Microelectronics (ITEM.me)
University of Bremen, Germany, 28359 Bremen, Otto-Hahn Allee 1
{schmale, lange, knoop, peters, steffen.paul}@me.uni-bremen.de

ABSTRACT

The aim of this study is to present the first compression and reconstruction methodology based on patch ordering inpainting algorithm for monitoring neural activity. This novel inpainting approach is especially important for the technical realization of implantable neural measurement systems (NMS) since they are subject to strict resource limitations as area and energy consumption. Intersection masks with center square as well as random-based masks are utilized for suitable neural data compression considering the patch ordering inpainting. The proposed inpainting methodology outperforms the structure-based inpainting algorithm and often applied Compressed Sensing strategy with regard to reconstruction quality of the real measured neural signals. These algorithms focus on complexity reduction according to hardware on implantable NMS. At high degrees of compression, the patch ordering inpainting yields well-suited or equal reconstruction results in contrast to JPEG or JPEG2000, respectively.

Index Terms— Patch Ordering inpainting, Mask, Neural Signals, Compression/Reconstruction, Permutation

1. INTRODUCTION AND RELATED WORK

Long term recording of brain activity is of growing interest for general research as well as medical diagnostics. The recorded neurological data is used in several applications like detection of epileptic seizures [1], controlling prosthetics [2] or to gain a better understanding of the function of the human brain. Traditional measurement equipment utilizes a wired connection between the electrodes and the recording equipment which forces the patient to stay close to the measurement setup. Since certain measurements for epileptic seizures can take days, this is a major inconvenience. In general measurements are performed using scalp electrodes placed on the head. Because of the electrode placement, these measurements are limited in spatial resolution. If a higher resolution is required, measurements are performed on an open skull using a multi-electrode-array (MEA) placed on the brain surface. Due to the open skull, this procedure poses a high risk for infections and can only be done in a clinical environment.

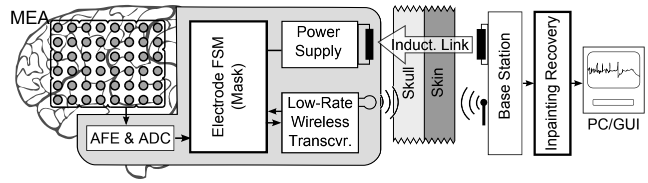

Fig. 1. Design of a NMS including an analog front-end (AFE), an analog-to-digital converter (ADC), a data compression unit (here a low area and low energy inpainting mask as FSM) and a low-rate wireless transceiver, modified from [4].

In order to alleviate these drawbacks, implantable neural measurement systems (NMS) have been developed. These implants (Tx) are placed below the skull and are capable of monitoring the brain activity, constantly. The MEA is placed on the brain surface enabling high spatial resolution. At the same time, the skull is closed without any physical connection, which eliminates the risk of infections and the need to stay inside a sterile environment. The recorded data is transmitted to an external base station (Rx) wirelessly, enabling remote diagnostics during everyday life of the patient. As there are no physical connections penetrating the skull, the energy supply has to work wirelessly as well. This severely restricts the available energy for the implant and requires all utilized components to work with a minimal amount of energy. Additionally, the heat dissipation of the implants components has to be low in order to prevent brain tissue damage caused by a localized rise in temperature [3].

Since the interpretation of neurological signals requires a high spatial and temporal resolution, MEA with up to 100 [5] and even 1000 [6] electrodes are used depending on the application. The temporal resolution is achieved with sampling rates of $15\,\mathrm{kHz}$ [7] or $30\,\mathrm{kHz}$ [8]. By quantizing with 10 bit [7], data rates of several Mbits are easily generated. Transceivers approved within the highly constrained environment of neurological implants currently do not provide enough communication bandwidth to transmit this amount of information. Consequently, this necessitates a data compression scheme. Standard methods like JPEG [9] are unfeasible in this application since the required calculation steps like transformation, quantization, coding etc. result in a high

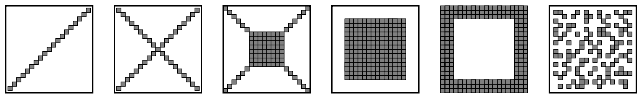

a.) dkkuuhr0 b.) dkkuuir0 c.) dkkuuip0 d.) rkkuubb0 e.) $\overline{\text{rkkuubb0}}$ f.) nkkuuc00

Fig. 2. Prime structures of different masks are shown, where activated samples (kk) are denoted with gray and deactivated regions (uu) with white: a.) Hatched ($hl0$), b.) Intersections ($ir0$) (c.) with center square ($ip0$)), d.)-e.) Rectangular ($bb0$) grid and f.) random mask ($c00$).

circuit complexity. Hence, special compression methods are needed with low complexity at the transmitter.

A possible solution is Compressed Sensing (CS) [10, 11], which has gained since attention among bio-medical applications due to its simple compression based on linear combinations. While the recovery is more complex, this effectively shifts computational complexity from the implant to the base-station. This characteristic to shift hardware complexity is called complexity reduction (CR). The integration of the CS strategy into analog-to-digital converters lead to promising hardware-based solutions in NMS [12].

This investigation offers insight into the introduction of a novel data compression and reconstruction methodology based on patch ordering inpainting. The applicability of structure-based inpainting [13] for neural signals has been shown in previous works [14] with suitable results.

2. PATCH ORDERING INPAINTING

The recovery process based on patch ordering inpainting [15] using permutation and interpolation is suited for especially sparse representations. Let $\mathbf{A} \in \mathbb{R}^{M \times N}$ be an array consisting of neural signals and $\mathbf{\Omega} \in \{0,1\}^{M \times N}$ be a logical matrix called *mask*, which distinguishes the retained regions (labeled by 1) from the corrupted/unknown parts (labeled by 0) in $\mathbf{A}$. The masked parts of the neural array $\mathbf{A}(\mathbf{\Omega}) = \mathbf{A} \wedge \mathbf{\Omega}$ are not transferred (data reduction) to the base station, where the mask $\mathbf{\Omega}$ also has to be known for the recovery. This leads to a NMS design with less circuit complexity, as shown in fig. 1.

In order to obtain multiple regular signals or rather piecewise constant signals for the reconstruction, N_p[1] overlapping patches of dimension $P \times P$ have to be extracted from $\mathbf{A}(\mathbf{\Omega})$, arranged in a vector and stored in a so-called patch collection matrix $\mathbf{C} \in \mathbb{R}^{P \cdot P \times N_p}$. The latter includes the known regions (information) of $\mathbf{A}$ and masked parts labeled by zero.

Furthermore, the reordering of the patches is accomplished by a permutation operator $\mathbf{p} \in [1, N_p]^{N_p}$. The sorting of the patches is essential for the algorithm and in addition computationally intensive. An approach which resembles the *cycle spinning* method [16] returns the permutation $\mathbf{p}$, which is used to improve the smoothness of the recorded neural array and to enhance the efficency.

[1]Number of extracted patches $N_p = (M - P + 1)(N - P + 1)$ in $\mathbf{C}$.

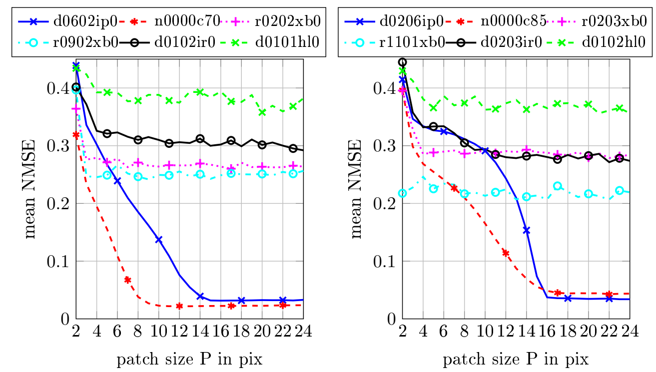

(a) Mean NMSE depending on patch size P for a given $\eta \approx 70\%$.

(b) Mean NMSE depending on patch size P for a given $\eta \approx 85\%$.

Fig. 3. Comparsion of inpainting recovery quality for different patch dimensions P and compression level η for N=128.

While only columns (vector version of the patches) of $\mathbf{C}$ are affected by the sorting due to the permutation $\mathbf{p}$, the rows represent the regular signals, which have to be individually interpolated. Therefore, the known parts of $\mathbf{A}(\mathbf{\Omega})$ in $\mathbf{C}$ act as the supporting points for a traditional 1D smoothing operator $\mathbf{H}$, e.g. *cubic spline* interpolation, which is applied to determine an estimation of the unknown parts in $\mathbf{A}(\mathbf{\Omega})$. After relocated the patches to their original positions, the arithmetic average has to be calculated for the overlapping parts. In order to improve the result of the inpainting reconstruction this process can be repeated by applying several permutation operators $\mathbf{p}_i$ in parallel fashion, where $1 \leq i \leq K$ holds.

3. MASK RESULTS

Concerning the implementation of a data compression scheme with regard to inpainting for neural signals on a fully implantable NMS, selected electrodes in the MEA have to be activated and deactivated in a specified manner. The spatial and time pattern in the neural array $\mathbf{A}$ is called mask $\mathbf{\Omega}$ and must be known on the Tx and Rx side, respectively. Only by transmitting the activated signal amplitudes at specific spatial and time samples, the data reduction can be realized.

Figure 2 shows the different types of masks which are analyzed in this work. Here, elementary parts of the individual masks including hatched, intersections, rectangular or random structures are visualized. In the interest of obtaining the global mask to indicate activated and deactivated electrodes for the neural recording, the prime structure has to be duplicated and placed side by side on the complete array $\mathbf{A}$.

As introduced in section 2, a quadratic overlapping sliding window called patch of dimension $P \times P$ is used for ordering and permutating in the reconstruction procedure in order to produce a smooth represenation of the neural array. The size P of the patch and shape of the used mask are crucial for the quality of the recovery. After having established two figures

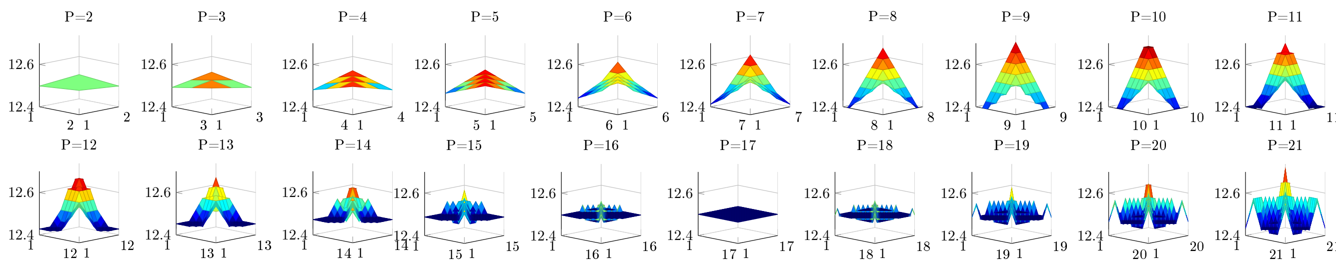

Fig. 4. Evolution of occurrence in $\%$ of the information content (entropy) of known data (z axis) depending on the quadratic patch of size $P \times P$ in pix (x-y-plane). Here, the mask $\mathbf{\Omega}_{\text{d0206ip0}}$ of dimension 48×128 and compression $\eta \approx 88\%$ is considered.

of merit used in all following examinations, the analysis of the different masks depending on the patch size will be executed.

In order to assess the suitability of the proposed recovery algorithm, the *normalized mean squared error* (NMSE)

$$\text{NMSE} = \frac{\|\mathbf{A}_0(\mathbf{\Omega}) - \hat{\mathbf{A}}(\mathbf{\Omega})\|_{\text{F}}}{\|\mathbf{A}_0(\mathbf{\Omega})\|_{\text{F}}}, \tag{1}$$

is utilized, where $\mathbf{A}_0(\mathbf{\Omega})$ stands for the original array and $\hat{\mathbf{A}}(\mathbf{\Omega})$ marks the recovery. The letter F in expression $\|\cdot\|_{\text{F}}$ denotes the *Frobenius* norm. By setting parts of $\mathbf{A}$ to zero due to the mask $\mathbf{\Omega}$, the *compression ratio* η can be defined by $\eta = 100\% \, [1 - |\mathbf{\Omega}|/(NM)]$, where M and N imply the dimension of $\mathbf{A}$ and $|\cdot|$ is the cardinality of $\mathbf{\Omega}$ which corresponces to the number of activated electrodes in the MEA.

Figure 3 presents the mean NMSE of the proposed inpainting-based data recovery approach as a function of the patch size P for the introduced types of mask $\mathbf{\Omega}$ and in addition two degrees of data reduction $\eta = \{70\%, 85\%\}$ for neural raw signals. With the exception of the intersection mask with center square and the random mask, the remaining mask types exhibit inadequate recovery results for arbitrary patch sizes. The reason of that are less connected regions as well as complete deactivated row/columns in $\mathbf{\Omega}$. In the case of lower η, fig. 3a, the mask $\mathbf{\Omega}_{\text{n0000c85}}$ based on a random distribution achieves more suitable NMSE compared to $\mathbf{\Omega}_{\text{d06s02ip0}}$ by reason of larger associated regions. The c85 for mask $\mathbf{\Omega}_{\text{n0000c85}}$ labels that 85% of the entries are set to zeros and d06 and s02 in mask $\mathbf{\Omega}_{\text{d06s02ip0}}$ denote the center square size and distance to each other, respectively. At higher compression ratios shown in fig. 3b, this issue is interchanged. Therefore, the intersection mask $\mathbf{\Omega}_{\text{d02s06ip0}}$ with center squares obtain better inpainting recovery results for neural signals compared to random implementations. In addition, they offer advantages in terms of implementation in resource-limited systems due to the uniform grid structure. Hence, intersection masks with center squares are used in all following simulations in sec. 4.

From a specific patch dimension (in fig. 3a $P \geq 16$) a convergence behavior of the NMSE can be observed, while increasing P, because the patch collection matrix $\mathbf{C}$ does not contain all zero columns due to the mask geomentry. The all zero columns corresponding to patches without known samples (information) deteriorate the results of the 1D smoothing operator $\mathbf{H}$, which does not lead to regular signals.

Figure 4 illustrates the histograms of the mean information content (entropy) of several patch sizes P for the mask $\mathbf{\Omega}_{\text{d0206ip0}}$ corresponding to a compression ratio of $\eta \approx 88\%$. The entropy denotes the occurrence of the known data at the individual positions in the sliding and overlapping patch in the reconstruction procedure of patch ordering inpainting. In the field of $2 \leq P \leq 15$ the histograms exhibit a strong dominant center peak. Thus, a lot of zero patches are included in $\mathbf{C}$, which leads to an inaccurate recovery results as observed in fig. 3b. From a patch dimension of $P \geq 16$ a low NMSE level is reached, because the all zero patches are not existing in the patch collection matrix $\mathbf{C}$ for the mask $\mathbf{\Omega}_{\text{d0206ip0}}$, which results in a more flat distribution of the mean patch information. This point is reached if $\mod(2(d+s), P) = 0$ holds. In order to weight the known data in a uniform fashion, patch dimension $P = 17$ is used in the following inpainting reconstruction simulations for neural signals.

4. SIMULATION RESULTS

The experimental results of the novel data compression and reconstruction methodology for neural signals based on the patch ordering inpainting algorithm are now shown in the following. For the inpainting recovery procedure a 1D smoothing by a cubic spline interpolation, two parallel permutation operations and a patch size of $P = 17$ are applied. To reduce the neural raw data on implant side, three masks $\mathbf{\Omega}$ with different center square sizes with regard to compression ratios of $\eta = \{70\%, 81\%, 88\%\}$ are applied in the simulation.

All simulation results presented in this paper include neural raw data, local field potentials (LFP), which were recorded invasively from a male epilepsy patient (human) by a surface MEA for 24h at the *Epilepsy Centre of Erlangen* (EZE) [17]. Each neural array $\mathbf{A} \in \mathbb{R}^{M \times N}$ contains M time signals with N samples recorded by M different electrodes. These data arrays were extracted from a 24h medical monitoring and sampled at $f_S = 1024\,\text{Hz}$ with a resolution of $16\,\text{bits}$.

CS [10] is implemented in this paper acting as a reference scheme to evaluate the novel inpainting methodology for

Table 1. NMSE of the patch ordering inpainting compared to CS, structure-based inpainting and JPEG for several given compression η applied on real measured neural data [17].

Method	$\overline{\text{NMSE}}$	$\sigma_{\overline{\text{NMSE}}}$	η	CR
struct. Inpainting [14]	0.078	± 0.012	62%	Yes
This Work ($\mathbf{\Omega}_{\text{d0602ip0}}$)	**0.035**	$\mathbf{\pm 0.008}$	**70%**	**Yes**
CS ($B = 39$)	0.343	± 0.105	70%	Yes
This Work ($\mathbf{\Omega}_{\text{d0404ip0}}$)	**0.036**	$\mathbf{\pm 0.007}$	**81%**	**Yes**
CS ($B = 24$)	0.550	± 0.099	81%	Yes
This Work ($\mathbf{\Omega}_{\text{d0206ip0}}$)	**0.038**	$\mathbf{\pm 0.009}$	**88%**	**Yes**
CS ($B = 16$)	0.747	± 0.094	88%	Yes
JPEG	0.133	± 0.019	88%	No
JPEG2000	0.034	± 0.005	88%	No

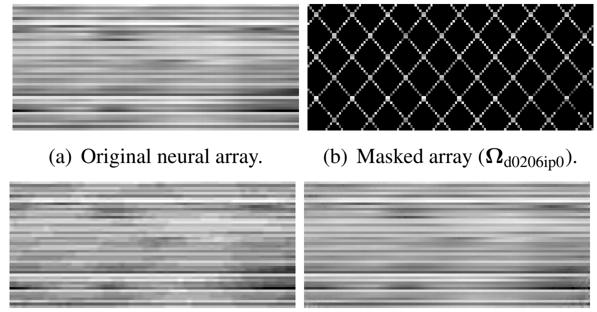

(a) Original neural array. (b) Masked array ($\mathbf{\Omega}_{\text{d0206ip0}}$).

(c) Result of JPEG2000. (d) Result of proposed inpainting.

Fig. 5. Different presentations of a single neural array $\mathbf{A}$ (x-axis: time, $N = 128$, y-axis: spatial, $M = 48$). The signal amplitudes are visualized in grayscale (black is zero value).

neural signal compression and reconstruction. Equivalent to the proposed inpainting approach, CS is suited for data compression in resource-limited systems like fully implantable NMS since both approaches focus on resource efficiency on implant side. This trait is labeled by complexity reduction (CR). The used CS framework utilizes a Gaussian-distributed incomplete system $\mathbf{\Phi} \in \mathbb{R}^{B \times N}$ to project the signal representations in $\mathbf{A}$ with time length N onto B observations. In the following simulations, $B = \{16, 24, 39\}$ is used to obtain the desired compression ratios. For the CS framework, η is defined as $\eta = 100\% \, [1 - B/N]$. Based on a sparsity-aware basis[2], sparse signal reconstruction can tractably be rendered by solving the ℓ_1-optimization problem using CVX [19].

Table 1 shows the average of the quality of reconstruction NMSE for several degrees of data compression η of the novel inpainting methodology and CS for a large number of neural signals. By comparing the compression/reconstruction schemes for neural raw data in resource-limited systems labeled by CR=Yes, the proposed inpainting approach outperforms CS reference framework in terms of NMSE. In addition, a structure-based inpainting has been applied from [14] consisting of a mask $\mathbf{\Omega}_{\text{o}}$ with overlapping rectangular patches to compress and recover neural raw data. In spite of compression ratio 62% less than 70%, the structure-based inpainting generates more than twice as the mean recovery error NMSE compared to the patch ordering inpainting algorithm. For the proposed inpainting based on patch ordering the enhancement of η only effects a small raise of the recovery error as expected, which yields benefits for high data compression ratios. The reconstruction results can be improved by increasing the spatial inter-electrode correlation of the neural signals due to correlation-based sorting of the neural array $\mathbf{A}$ in order to increase the image-related structure [4, 14]. With respect to traditional data compression schemes like JPEG, which are unfeasible for resource-limited systems labeled by CR=No, the introduced inpainting method also yields well-suited results. While standard JPEG is less effective to compress and recover neural signals at a compression ratio of 88%, JPEG2000 and the proposed inpainting methodology achieves similar recovery quality of less than 4% NMSE.

Figure 5c and 5d visualize the differences of JPEG2000 and inpainting recovery for a neural array at $\eta \approx 88\%$ and $\text{NMSE} < 4\%$ compared to tab. 1. For JPEG2000 recovery a large amount of artifacts due to the quantization of the block-based DCT can be observed. The neural array reconstruction of the inpainting methodology exhibits less artifacts as well as more regular signals representation and owns the benefits of complexity reduction on implant side.

5. CONCLUSION

This paper introduces the patch ordering inpainting as a well-suited data compression and reconstruction methodology for neural signals for the first time. This Work focuses on transfering the complexity from implant to base-station in resource-limited systems. In fully implantable NMS, this leads to a benefit in terms of area and energy consumption. The quality of the recovery as well as the degree of compression strongly depend on the selected inpainting mask. The evaluation shows that this intersection mask with center squares is well-suited for the data reduction and reconstruction of neural signals. Thereby, the proposed patch ordering inpainting algorithm achieves promising results, especially when compared to the structure-based inpainting or the Compressed Sensing strategy using CVX. At identical compression ratios, the proposed inpainting approach clearly outperforms the CS strategy in terms of reconstruction accuracy. Even the results of traditional techniques like JPEG2000 can be achieved for large degrees of compression without recovery artifactes by the promising inpainting methodology, which inherits in addition the benefits of reduction of complexity for resource-limited systems.

[2]Discrete cosine transform (DCT) is used as basis in this paper [18].

6. REFERENCES

[1] R. Meier, H. Dittrich, A. Schulze-Bonhage, and A. Aertsen, "Detecting epileptic seizures in long-term human eeg: A new approach to automatic online and real-time detection and classification of polymorphic seizure patterns," *Journal of Clinical Neurophysiology*, vol. 25, no. 3, 2008.

[2] P. Shenoy, K.J. Miller, J.G. Ojemann, and R.P.N. Rao, "Generalized features for electrocorticographic bcis," *Biomedical Engineering, IEEE Transactions on*, vol. 55, no. 1, pp. 273–280, Jan 2008.

[3] S. Kim, P. Tathireddy, R.A. Normann, and F. Solzbacher, "Thermal impact of an active 3-d microelectrode array implanted in the brain," *Neural Systems and Rehabilitation Engineering, IEEE Transactions on*, vol. 15, no. 4, pp. 493–501, 12 2007.

[4] S. Schmale, J. Hoeffmann, B. Knoop, G. Kreiselmeyer, H. Hamer, D. Peters-Drolshagen, and S. Paul, "Exploiting correlation in neural signals for data compression," in *Signal Processing Conference (EUSIPCO), 2014 Proceedings of the 22nd European*, Sept 2014, pp. 2080–2084.

[5] J. Pistor, J. Hoeffmann, D. Rotermund, E. Tolstosheeva, T. Schellenberg, D. Boll, V. Gordillo-Gonzalez, S. Mandon, D. Peters-Drolshagen, A. Kreiter, M. Schneider, W. Lang, K. Pawelzik, and S. Paul, "Development of a fully implantable recording system for ecog signals," in *Design, Automation Test in Europe Conference Exhibition (DATE), 2013*, March 2013, pp. 893–898.

[6] K.D. Wise, D.J. Anderson, J.F. Hetke, D.R. Kipke, and K. Najafi, "Wireless implantable microsystems: high-density electronic interfaces to the nervous system," *Proceedings of the IEEE*, Jan. 2004.

[7] R.R. Harrison, "The design of integrated circuits to observe brain activity," *Proceedings of the IEEE*, vol. 96, no. 7, pp. 1203–1216, 7 2008.

[8] B. Gosselin, A.E. Ayoub, J.-F. Roy, M. Sawan, F. Lepore, A. Chaudhuri, and D. Guitton, "A mixed-signal multichip neural recording interface with bandwidth reduction," *Biomedical Circuits and Systems, IEEE Transactions on*, vol. 3, no. 3, pp. 129–141, 6 2009.

[9] G.K. Wallace, "The jpeg still picture compression standard," *Consumer Electronics, IEEE Transactions on*, vol. 38, no. 1, pp. xviii–xxxiv, Feb 1992.

[10] E.J. Candes, J. Romberg, and T. Tao, "Robust uncertainty principles: exact signal reconstruction from highly incomplete frequency information," *Information Theory, IEEE Transactions on*, 2006.

[11] E.J. Candes and J. Romberg, "Sparsity and incoherence in compressive sampling," *Inverse problems*, vol. 23, no. 3, 2006.

[12] H. Lange, S. Schmale, B. Knoop, D. Peters-Drolshagen, and S. Paul, "ADC topology based on compressed sensing for low power brain monitoring," *Procedia Engineering*, vol. 120, pp. 315 – 319, 2015, Eurosensors 2015.

[13] M. Bertalmio, G. Sapiro, V. Caselles, and C. Ballester, "Image inpainting," in *Proceedings of the 27th Annual Conference on Computer Graphics and Interactive Techniques*, New York, NY, USA, 2000, SIGGRAPH '00, ACM Press/Addison-Wesley Publishing Co.

[14] S. Schmale, B. Knoop, D. Peters-Drolshagen, and S. Paul, "Structure reconstruction of correlated neural signals based on inpainting for brain monitoring," in *Biomedical Circuits and Systems Conference (BioCAS), 2015 IEEE*, Oct 2015, pp. 1–4.

[15] I. Ram, M. Elad, and I. Cohen, "Image processing using smooth ordering of its patches," *CoRR*, vol. abs/1210.3832, 2012.

[16] R. R. Coifman and D. L. Donoho, "Translation-invariant de-noising," 1995, pp. 125–150, Springer-Verlag.

[17] Epilepsy Centre of Erlangen (EZE) Germany, "Data of the Epilepsy Centre," 2013, http://www.epilepsiezentrum.uk-erlangen.de/.

[18] S. Schmale, B. Knoop, J. Hoeffmann, D. Peters-Drolshagen, and S. Paul, "Joint compression of neural action potentials and local field potentials," in *Signals, Systems and Computers, 2013 Asilomar Conference on*, Nov 2013, pp. 1823–1827.

[19] CVX Research Inc., "CVX: Matlab software for disciplined convex programming, version 2.0 beta," 2012.